

Exact solutions for spine reconnection magnetic annihilation

BY C. MELLOR^a, E. R. PRIEST^a AND V. S. TITOV^b

^a*Applied Mathematics Division, St Andrews University, St Andrews KY16 9SS,
UK,* ^b*Theoretische Physik IV, Ruhr-Universität Bochum, 44780 Bochum,
Germany*

Solutions for spine reconnection annihilation are presented which satisfy exactly the three-dimensional equations of steady-state resistive incompressible magnetohydrodynamics (MHD). The magnetic flux function (A) and stream function (Ψ) have the form

$$A = A_0(R) \sin \phi + A_1(R)z, \quad \Psi = \Psi_0(R) \sin \phi + \Psi_1(R)z,$$

in terms of cylindrical polar coordinates (R, ϕ, z) . First of all, two nonlinear fourth-order equations for A_1 and Ψ_1 are solved by the method of matched asymptotic expansions when the magnetic Reynolds number is much larger than unity. The solution, for which a composite asymptotic expansion is given in closed form, possesses a weak boundary layer near the spine ($R = 0$). These solutions are used to solve the remaining two equations for A_0 and Ψ_0 . Physically, the magnetic field is advected across the fan separatrix surface and diffuses across the spine curve. Different members of a family of solutions are determined by values of a free parameter (γ) and the components (B_{Re}, B_{ze}) and (v_{Re}, v_{ze}) of the magnetic field and plasma velocity at a fixed external point $(x, y, z) = (0, 1, 0)$, say.

1 Introduction

Magnetic reconnection is a basic process that is responsible for many dynamic processes in laboratory, space, solar and astrophysical plasmas. The theory of two-dimensional reconnection is now well developed and most of the current interest has turned to beginning to address the three-dimensional problem (Priest & Forbes, 2000), which has many different aspects, (eg. Lau & Finn, 1990, Schindler *et al*, 1988, Hornig & Rastätter, 1998).

Exact solutions to the MHD equations for magnetic annihilation in two and three dimensions were first discovered by Sonnerup & Priest (1975), in which a stagnation-point flow carries straight field lines into a one-dimensional current sheet

where the magnetic field diffuses through the plasma. The two-dimensional model was generalised by Craig & Henton (1995) to give solutions for two-dimensional reconnective annihilation, in which the magnetic field lines have an X-type topology but the electric current is one-dimensional and the field lines diffuse across the separatrix along which the current lies. These solutions were themselves generalised further in a two-fold manner by Priest *et al* (2000).

Reconnection in three dimensions occurs at a null point in a combination of two ways (Priest & Titov, 1996). *Spine reconnection* takes place when the current, and therefore the magnetic dissipation, concentrates along an isolated field line (called the spine) that goes to or from the null. *Fan reconnection* takes place when the current concentrates instead in a surface of field lines (called the fan) that go to or from the null in the opposite sense to the spine.

Craig *et al* (1995) discovered an exact solution for reconnective fan annihilation, which consists of a three-dimensional sheared stagnation-point flow of the form

$$v_x = -x, \quad v_y = Ky - F_y(x), \quad v_z = (1 - K)z - F_z(x),$$

with a magnetic field

$$\mathbf{B} = \lambda \mathbf{v} + G_y(x)\hat{\mathbf{y}} + G_z(x)\hat{\mathbf{z}}.$$

In this regime,

$$\mathbf{F} = -\frac{\lambda}{1 - \lambda^2} \mathbf{G},$$

and the functions $G_y(x)$ and $G_z(x)$ are given by solving

$$xG'_y + KG_y = -\frac{\eta}{1 - \lambda^2}G''_y,$$

$$xG'_z + (1 - K)G_z = -\frac{\eta}{1 - \lambda^2}G''_z.$$

where $G' \equiv dG/dx$.

Craig & Fabling (1996) also discovered solutions for spine reconnective annihilation which can be written in cylindrical polar coordinates (R, ϕ, z) in the form

$$v_z = -2z + \lambda f(R) \cos(m\phi), \quad v_R = R, \quad (1)$$

$$B_z = -2\lambda z + f(R) \cos(m\phi), \quad B_R = \lambda R, \quad (2)$$

where $f(R)$ satisfies

$$2f + Rf' = \frac{\eta}{1 - \lambda^2} \left(f'' + \frac{f'}{R} - \frac{m^2 f}{R^2} \right), \quad (3)$$

and in this case, $f' \equiv df/dR$. Flow across the fan produces a cylindrical diffusion region of radius $\sim \eta^{1/2}$ with a linearly increasing field surrounding the spine, outside which the field falls off as R^{-2} .

The purpose of the present article is to present some new exact solutions for spine reconnective annihilation that are much more general than the previous Craig-Fabring solutions and to find explicit expressions for them to leading order in η . After presenting the basic equations and the form for the new solutions in terms of the variables A_1, Ψ_1, A_0 and Ψ_0 (Section 2), we change the variables to $(a_1, \psi_1, a_0, \psi_0, s)$ to simplify the equations. In section 3 we give the boundary-layer solutions of the nonlinear equations for a_1 and ψ_1 , while in section 4 we use the solutions found in section 3 to solve the equations for a_0 and ψ_0 . The basic properties of the solutions are developed in sections 5 and 6.

2 Form for new exact solutions

2.1 Basic equations

The basic MHD equations for steady incompressible three-dimensional flow are the induction equation,

$$\nabla \times (\mathbf{v} \times \mathbf{B}) + \eta \nabla^2 \mathbf{B} = \mathbf{0} \quad (4)$$

and the equation of motion

$$\rho(\mathbf{v} \cdot \nabla)\mathbf{v} = -\nabla \left(p + \frac{B^2}{2\mu} \right) + (\mathbf{B} \cdot \nabla) \frac{\mathbf{B}}{\mu}, \quad (5)$$

where

$$\nabla \cdot \mathbf{B} = \nabla \cdot \mathbf{v} = 0, \quad (6)$$

in terms of the magnetic field \mathbf{B} and the plasma velocity \mathbf{v} . The plasma density (ρ) and magnetic diffusivity (η) are assumed uniform and the electric current is

$$\mathbf{j} = \frac{1}{\mu} \nabla \times \mathbf{B}.$$

The equations (6) may be satisfied identically by writing the velocity and magnetic field in terms of the flux function (A) and stream function (Ψ) as

$$\mathbf{B} = -\nabla \times (A\hat{\phi}), \quad \mathbf{v} = -\nabla \times (\Psi\hat{\phi}).$$

In what follows we set $L_e = 1, \mu = 1, \rho = 1$ without loss of generality, since this is equivalent to rescaling distances with respect to the distance (L_e) from the origin at which $v = v_e$, rescaling the density with respect to ρ and absorbing μ in \mathbf{B} .

2.2 Proposed new solutions

The form for the new solutions that we seek in cylindrical polar coordinates (R, ϕ, z) is

$$A = A_0(R) \sin \phi + A_1(R)z, \quad \Psi = \Psi_0(R) \sin \phi + \Psi_1(R)z,$$

with four free functions of R . The corresponding magnetic field and velocity are

$$\mathbf{B} = -\nabla \times (A\hat{\phi}), \quad \mathbf{v} = -\nabla \times (\Psi\hat{\phi}),$$

and have components

$$B_R = A_1, \quad B_\phi = 0, \quad B_z = -\dot{A}_0 \sin \phi - \dot{A}_1 z, \quad (7)$$

$$v_R = \Psi_1, \quad v_\phi = 0, \quad v_z = -\dot{\Psi}_0 \sin \phi - \dot{\Psi}_1 z, \quad (8)$$

where $\dot{f} \equiv R^{-1}d(Rf)/dR$.

The steady state induction equation (4) and the curl of the momentum equation (5) can be used to show that

$$A_1 \dot{\Psi}_1 - \Psi_1 \dot{A}_1 + \eta \frac{d\dot{A}_1}{dR} = 0, \quad (9)$$

$$-(\dot{\Psi}_1)^2 + \Psi_1 \frac{d\dot{\Psi}_1}{dR} + (\dot{A}_1)^2 - A_1 \frac{d\dot{A}_1}{dR} = -k, \quad (10)$$

$$\left(A_1 \dot{\Psi}_0 - \Psi_1 \dot{A}_0 + \eta \frac{d\dot{A}_0}{dR} \right)' = \frac{\eta}{R^2} \dot{A}_0, \quad (11)$$

$$\Psi_1 \frac{d\dot{\Psi}_0}{dR} - \dot{\Psi}_0 \dot{\Psi}_1 - A_1 \frac{d\dot{A}_0}{dR} + \dot{A}_0 \dot{A}_1 = 0, \quad (12)$$

where k is a constant of integration. There are eight natural boundary conditions that we impose, namely, $\mathbf{B} = \mathbf{v} = \mathbf{0}$ at the origin and $\mathbf{B} = \mathbf{B}_e$ and $\mathbf{v} = \mathbf{v}_e$ at the external point $(x, y, z) = (0, 1, 0)$ or, in terms of the flux function and stream function, $A_1(0) = \Psi_1(0) = 0$, $A_1(1) = B_{Re}$, $\Psi_1(1) = v_{Re}$, $\dot{A}_0(0) = \dot{\Psi}_0(0) = 0$, $\dot{A}_0(1) = -B_{ze}$ and $\dot{\Psi}_0(1) = -v_{ze}$.

These equations simplify greatly by making the substitutions $a = RA$, $\psi = R\Psi$ and $s = R^2/2$, for which the equations become

$$a_1 \frac{d\psi_1}{ds} - \psi_1 \frac{da_1}{ds} + 2\eta s \frac{d^2 a_1}{ds^2} = 0, \quad (13)$$

$$-\left(\frac{d\psi_1}{ds}\right)^2 + \psi_1 \frac{d^2\psi_1}{ds^2} + \left(\frac{da_1}{ds}\right)^2 - a_1 \frac{d^2a_1}{ds^2} = -k, \quad (14)$$

$$\frac{d}{ds} \left(a_1 \frac{d\psi_0}{ds} - \psi_1 \frac{da_0}{ds} + 2\eta s \frac{d^2a_0}{ds^2} \right) = \frac{\eta}{2s} \frac{da_0}{ds}, \quad (15)$$

$$\psi_1 \frac{d^2\psi_0}{ds^2} - \frac{d\psi_0}{ds} \frac{d\psi_1}{ds} - a_1 \frac{d^2a_0}{ds^2} + \frac{da_0}{ds} \frac{da_1}{ds} = 0. \quad (16)$$

The boundary conditions are now $a_1(0) = \psi_1(0) = 0$, $a_1(1/2) = B_{Re}$, $\psi_1(1/2) = v_{Re}$, $(da_0/ds)(0) = (d\psi_0/ds)(0) = 0$, $(da_0/ds)(1/2) = -B_{ze}$ and $(d\psi_0/ds)(1/2) = -v_{ze}$.

3 Solution for a_1 and ψ_1

We seek the solution of (13) and (14) subject to the given boundary conditions by using the method of matched asymptotic expansions, with an outer solution over most of the range ($0 < s \leq 1/2$) and an inner (boundary-layer) solution near $s = 0$. We are able to show that the outer solution is a uniformly valid solution to leading order for all s in the range $0 \leq s \leq 1/2$. A Taylor-series expansion about $s = 0$ gives

$$a_1 = a_{11}s + a_{14}s^4 + a_{15}s^5 + \dots,$$

$$\psi_1 = \psi_{11}s + \psi_{13}s^3 + \psi_{14}s^4 + \psi_{15}s^5 + \dots,$$

which is used later to start the numerical integration of the equations from $s = 0$. The inner boundary condition results in the coefficients $a_{12} = a_{13} = \psi_{12} = 0$ for the relevant terms in s^2 and s^3 . The absence of these terms in the Taylor expansions implies that $d^3a_1/ds^3(0) \equiv 0$. Also, substitution into the differential equations gives the relation $a_{11}^2 - \psi_{11}^2 = -k$.

3.1 Outer solution

The outer solution can be obtained by expanding in powers of η and matching terms of the same order in η . The first of these terms can be found by setting $\eta = 0$ in (13), giving

$$a_1^2 \frac{d}{ds} \left(\frac{\psi_1}{a_1} \right) = 0,$$

which may be integrated using the outer boundary conditions to give

$$\psi_1 = \frac{v_{Re}}{B_{Re}} a_1. \quad (17)$$

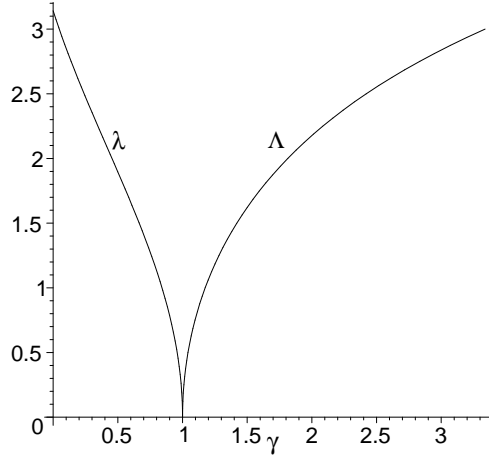


Figure 1: The variation of λ and Λ with the parameter γ .

Eliminating ψ_1 from (14) gives a second-order equation in a_1 that may be solved to give three different forms for the solution depending on the values of a positive parameter, γ , in terms of which

$$k = \frac{4(v_{Re}^2 - B_{Re}^2)}{\gamma^2} > 0. \quad (18)$$

If $\gamma = 1$, we have

$$a_1 = 2B_{Re}s, \quad \psi_1 = 2v_{Re}s. \quad (19)$$

If $\gamma < 1$, then by using a new parameter, λ , such that $(\sin \lambda)/\lambda = \gamma$, we obtain

$$a_1 = B_{Re} \frac{\sin(2\lambda s)}{\sin \lambda}, \quad \psi_1 = v_{Re} \frac{\sin(2\lambda s)}{\sin \lambda}, \quad (20)$$

If $\gamma > 1$, then

$$a_1 = B_{Re} \frac{\sinh(2\Lambda s)}{\sinh \Lambda}, \quad \psi_1 = v_{Re} \frac{\sinh(2\Lambda s)}{\sinh \Lambda}, \quad (21)$$

where the new parameter, Λ , is such that $(\sinh \Lambda)/\Lambda = \gamma$.

The variation of λ and Λ with γ is shown in figure 1.

The solutions (20), (19) and (21) satisfy, for any value of γ , both the outer and the inner boundary conditions. However, if $\gamma \neq 1$, they do not satisfy the full equations (13) and (14) with $\eta \neq 0$. For example, they have $d^3 a_1/ds^3(0) \neq 0$, whereas we saw from the series expansion about $s = 0$ that $d^3 a_1/ds^3(0) \equiv 0$. Hence a boundary layer near the origin is needed to bring $d^3 a_1/ds^3$ down to zero as the origin is approached and so accommodate this implicit boundary condition.

3.2 Inner solution

The boundary-layer equations are obtained by rescaling the dependent and independent variables in (13) and (14) in the following way

$$a_1 = \eta \bar{a}_1, \quad \psi_1 = \eta \bar{\psi}_1, \quad s = \eta \bar{s}. \quad (22)$$

The resulting equations in place of (13) and (14) are

$$\bar{a}_1 \bar{\psi}_1' - \bar{\psi}_1 \bar{a}_1' + 2\bar{s} \bar{a}_1'' = 0, \quad (23)$$

and

$$-(\bar{\psi}_1')^2 + \bar{\psi}_1 \bar{\psi}_1'' + (\bar{a}_1')^2 - \bar{a}_1 \bar{a}_1'' = -k, \quad (24)$$

where $f' \equiv df/d\bar{s}$. The boundary conditions for the inner solution become $\bar{a}_1(0) = 0$, $\bar{\psi}_1(0) = 0$, $\bar{a}_1'''(0) = 0$ and $\bar{\psi}_1'''(0) = 6\eta^2\psi_{13}$.

Setting

$$\bar{a}_1 = a_{11}\bar{s} + \eta^2\tilde{a}_1, \quad \bar{\psi}_1 = \psi_{11}\bar{s} + \eta^2\tilde{\psi}_1,$$

and substituting into (23) and (24) reduces them to a pair of linear equations

$$a_{11}(\bar{s}\tilde{\psi}_1' - \tilde{\psi}_1) - \psi_{11}(\bar{s}\tilde{a}_1' - \tilde{a}_1) - 2\bar{s}\tilde{a}_1'' = 0, \quad (25)$$

and

$$\psi_{11}(\bar{s}\tilde{\psi}_1'' - 2\tilde{\psi}_1') - a_{11}(\bar{s}\tilde{a}_1'' - 2\tilde{a}_1') = 0, \quad (26)$$

for which the boundary conditions are

$$\tilde{a}_1(0) = \tilde{\psi}_1(0) = \tilde{a}_1'(0) = \tilde{\psi}_1'(0) = 0, \quad \tilde{\psi}_1'''(0) = 6\psi_{13}.$$

Equation (26) can be integrated twice to give

$$\psi_{11}\tilde{\psi}_1 - a_{11}\tilde{a}_1 = \psi_{11}\psi_{13}\bar{s}^3. \quad (27)$$

Using this to eliminate $\tilde{\psi}_1$ from (25) and with $\sigma^2 = -k/\psi_{11}$, we then find

$$2\bar{s}\tilde{a}_1'' + \sigma^2(\bar{s}\tilde{a}_1' - \tilde{a}_1) + 2a_{11}\psi_{13}\bar{s}^3 = 0. \quad (28)$$

This can be manipulated to yield

$$\frac{d}{d\bar{s}} \left(\frac{\tilde{a}_1}{\bar{s}} \right) = -a_{11}\psi_{13} \frac{1}{\bar{s}^2} \exp\left(-\frac{\sigma^2}{2}\bar{s}\right) \int_0^{\bar{s}} t^3 \exp\left(\frac{\sigma^2}{2}t\right) dt, \quad (29)$$

which may be integrated to give an explicit solution for \tilde{a}_1 .

Expanding for small \bar{s} gives

$$\bar{a}_1 = -\frac{a_{11}\psi_{13}}{12}\bar{s}^4 + \dots,$$

$$\bar{\psi}_1 = \psi_{13}\bar{s}^3 - \frac{a_{11}^2\psi_{13}}{12\psi_{11}}\bar{s}^4 + \dots.$$

Expanding instead for large \bar{s} gives

$$\bar{a}_1 = -\frac{a_{11}\psi_{13}}{\sigma^2}\bar{s}^3 + \frac{12a_{11}\psi_{13}}{\sigma^4}\bar{s}^2 + O(\bar{s}\log(\bar{s})),$$

$$\bar{\psi}_1 = \psi_{13}\left(1 - \frac{a_{11}^2}{\sigma^2\psi_{11}}\right)\bar{s}^3 - \frac{12a_{11}^2\psi_{13}}{\sigma^4\psi_{11}}\bar{s}^2 + O(\bar{s}\log(\bar{s})).$$

3.3 Matching

In order to match the inner and outer solutions (29) and (20), (19) and (21), we now express the inner solution in terms of the outer variable (s) and expand for small η , so that

$$a_1 = a_{11}s - \frac{a_{11}\psi_{13}}{\sigma^2}s^3 + O(\eta). \quad (30)$$

Similarly, we expand the outer solution in terms of the inner variable for small η . When $\gamma < 1$ we obtain

$$a_1 = \frac{2\lambda B_{Re}}{\sin \lambda}s - \frac{4\lambda^3 B_{Re}}{3\sin \lambda}s^3 + \dots \quad (31)$$

Clearly the two solutions (30) and (31) can be matched provided

$$a_{11} = \frac{2\lambda B_{Re}}{\sin \lambda}, \quad \psi_{13} = -\frac{2\lambda^2 k}{3\psi_{11}}.$$

The outer solution (20) represents a composite solution to leading order.

When $\gamma > 1$, the same solution is obtained but with λ and λ^2 replaced by Λ and $(-\Lambda^2)$ respectively. Finally, when $\gamma = 1$ we find that the solution $a_1 = 2B_{Re}s$ is valid everywhere.

The numerical solutions for a_1 and ψ_1 to the full equations (13) and (14) are shown in figure 2, which gives the $\gamma < 1$ solutions with $\eta = 0.01$, $B_{Re} = 2$, $\lambda = 2$ and $k = 500$. The top part of figure 3 shows the boundary layer for $\eta = 0.01$ with the inner solution (dotted line) and the outer solution (dashed line) imposed over the numerical solution (solid line). The bottom part shows that the boundary layer varies in width for different values of η . The lowest curve is for $\eta = 0.001$, the next two curves are for $\eta = 0.003$ and $\eta = 0.01$ and the uppermost curve is for $\eta = 0.03$. The width of the boundary layer in each case is approximately η .

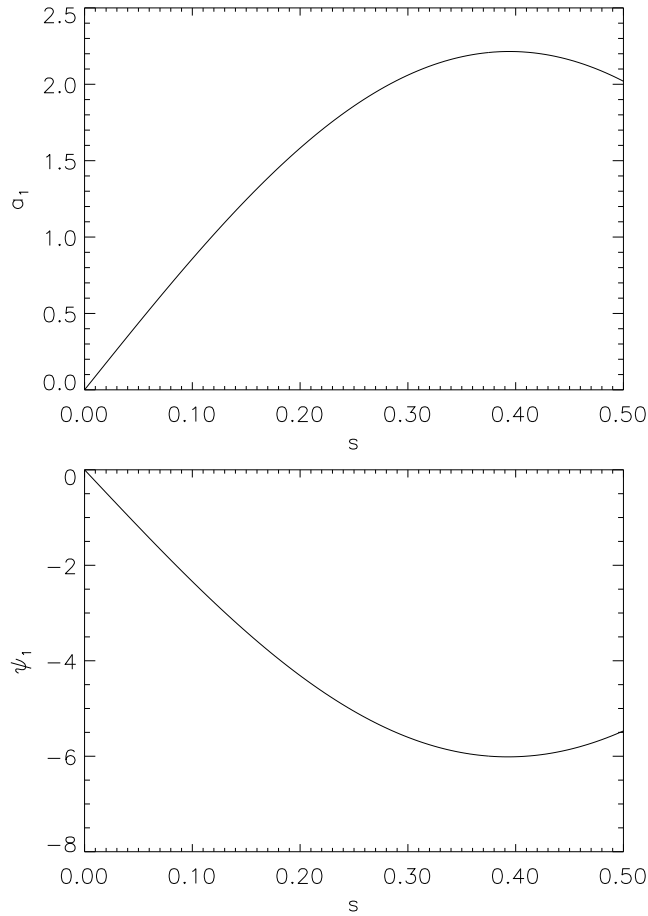


Figure 2: (Top) a_1 as a function of s for $\eta = 0.01$, $B_{Re} = 2$, $\lambda = 2$ and $k = 500$. (Bottom) ψ_1 as a function of s for $\eta = 0.01$, $B_{Re} = 2$, $\lambda = 2$ and $k = 500$.

4 Solution for a_0 and ψ_0

Having found the solutions to leading order for a_1 and ψ_1 , we now seek the solution of (15) and (16) for $a_0(s)$ and $\psi_0(s)$ subject to the conditions that $(da_0/ds)(0) = (d\psi_0/ds)(0) = 0$.

Again, solving the equations by the method of matched asymptotic expansions, we start with the Taylor-series expansions for a_0 and ψ_0 . These are

$$a_0 = a_{00} + a_{03}s^3 + a_{04}s^4 + \dots ,$$

$$\psi_0 = \psi_{00} + \psi_{02}s^2 + \psi_{03}s^3 + \psi_{04}s^4 + \dots .$$

We set a_{00} and ψ_{00} to zero to avoid a singularity at $R = 0$ when we change back to the original coordinates. All the other coefficients can be found in terms of ψ_{02} and the coefficients a_{11} and ψ_{13} of the Taylor series for a_1 and ψ_1 .

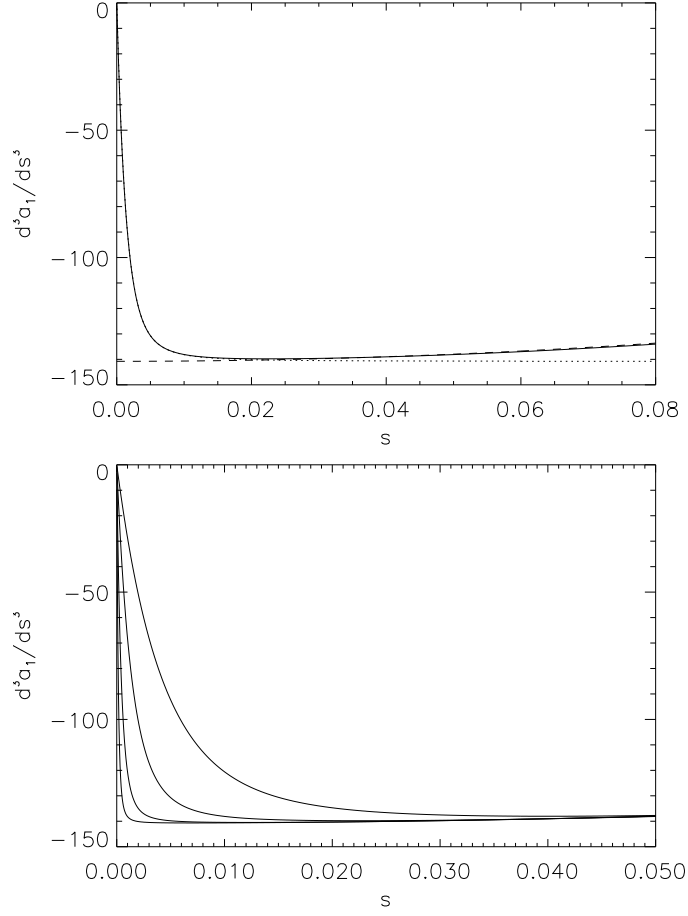


Figure 3: (*Top*) d^3a_1/ds^3 as a function of s shows the boundary-layer nature of the solution. The solid curve is the full numerical solution, the dashed curve is the outer solution and the dotted curve the inner solution. (*Bottom*) d^3a_1/ds^3 as a function of s for the values $\eta = 0.001, 0.003, 0.01$ and 0.03 that increase from left to right as the width of the boundary layer increases. All other parameters are as in figure 2.

4.1 Outer solution

To find the solution to leading order, again we set $\eta = 0$ and obtain

$$\frac{d}{ds} \left(a_1 \frac{d\psi_0}{ds} - \psi_1 \frac{da_0}{ds} \right) = 0.$$

After integrating and using the boundary conditions for a_1 and ψ_1 this becomes

$$a_1 \frac{d\psi_0}{ds} - \psi_1 \frac{da_0}{ds} = 0,$$

which gives

$$\frac{d\psi_0}{ds} = \frac{\psi_1}{a_1} \frac{da_0}{ds} = \frac{v_{Re}}{B_{Re}} \frac{da_0}{ds}.$$

Eliminating $d\psi_0/ds$ from (16) with $\gamma < 1$ we find

$$\frac{d^2 a_0}{ds^2} \sin(2\lambda s) - 2\lambda \frac{da_0}{ds} \cos(2\lambda s) = 0. \quad (32)$$

Integrating this and applying the outer boundary conditions, $(da_0/ds)(1/2) = -B_{ze}$ and $(d\psi_0/ds)(1/2) = -v_{ze}$ produces

$$\frac{da_0}{ds} = -\frac{B_{ze} \sin(2\lambda s)}{\sin \lambda}, \quad \frac{d\psi_0}{ds} = -\frac{v_{ze} \sin(2\lambda s)}{\sin \lambda}, \quad (33)$$

and so, after integrating,

$$a_0 = \frac{B_{ze}}{2\lambda \sin \lambda} (\cos(2\lambda s) - 1), \quad \psi_0 = \frac{v_{ze}}{2\lambda \sin \lambda} (\cos(2\lambda s) - 1). \quad (34)$$

When $\gamma = 1$, we obtain

$$a_0 = -B_{ze} s^2, \quad \psi_0 = -v_{ze} s^2. \quad (35)$$

When $\gamma > 1$ we find instead

$$a_0 = -\frac{B_{ze}}{2\Lambda \sinh \Lambda} (\cosh(2\Lambda s) - 1), \quad \psi_0 = -\frac{v_{ze}}{2\Lambda \sinh \Lambda} (\cosh(2\Lambda s) - 1). \quad (36)$$

Again, we choose $a_0(0) = \psi_0(0) = 0$ to avoid a singularity at $R = 0$ in the original coordinates.

4.2 Inner solution

Again, setting $a = \eta \bar{a}$, $\psi = \eta \bar{\psi}$ and $s = \eta \bar{s}$, equations (15) and (16) imply

$$\left(\bar{a}_1 \bar{\psi}_0' - \bar{\psi}_1 \bar{a}_0' + 2\bar{s} \bar{a}_0'' \right)' = \frac{\bar{a}_0'}{2\bar{s}}, \quad (37)$$

and

$$\bar{\psi}_1 \bar{\psi}_0'' - \bar{\psi}_0' \bar{\psi}_1' - \bar{a}_1 \bar{a}_0'' + \bar{a}_0' \bar{a}_1' = 0, \quad (38)$$

with boundary conditions $\bar{a}_0'(0) = \bar{\psi}_0'(0) = 0$, $\bar{a}_0''(0) = 0$ and $\bar{\psi}_0''(0) = 2\eta\psi_{02}$.

Again, $x' \equiv dx/d\bar{s}$.

Then putting

$$\begin{aligned} \bar{a}_0 &= \eta \tilde{a}_0, & \bar{\psi}_0 &= \eta \tilde{\psi}_0, \\ \bar{a}_1 &= a_{11} \bar{s} + \eta^2 \tilde{a}_1, & \bar{\psi}_1 &= \psi_{11} \bar{s} + \eta^2 \tilde{\psi}_1, \end{aligned}$$

we obtain the linear equations

$$\left(a_{11} \bar{s} \tilde{\psi}_0' - \psi_{11} \bar{s} \tilde{a}_0' + 2\bar{s} \tilde{a}_0'' \right)' = \frac{\tilde{a}_0'}{2\bar{s}}, \quad (39)$$

and

$$\psi_{11}\bar{s}\tilde{\psi}_0'' - \psi_{11}\tilde{\psi}_0' - a_{11}\bar{s}\tilde{a}_0'' + a_{11}\tilde{a}_0' = 0. \quad (40)$$

Integrating (40) and using the boundary conditions $\tilde{a}_0'' = 0$ and $\tilde{\psi}_0'' = 2\psi_{02}$ gives the relation

$$\psi_{11}\tilde{\psi}_0' - a_{11}\tilde{a}_0' = 2\psi_{11}\psi_{02}\bar{s}. \quad (41)$$

Using it to eliminate $\tilde{\psi}_0'$ from equation (39) we find

$$4\bar{s}^2\tilde{a}_0''' + (2\sigma^2\bar{s}^2 + 4\bar{s})\tilde{a}_0'' + (2\sigma^2\bar{s} - 1)\tilde{a}_0' = -8a_{11}\psi_{02}\bar{s}^2, \quad (42)$$

where $\sigma^2 = -k/\psi_{11}$ as before.

Solving for small \bar{s} gives

$$\tilde{a}_0 = -\frac{8a_{11}\psi_{02}}{45}\bar{s}^3 + \dots,$$

and

$$\tilde{\psi}_0 = \psi_{02}\bar{s}^2 - \frac{8a_{11}^2\psi_{02}}{45\psi_{11}}\bar{s}^3 + \dots$$

Solving for large \bar{s} gives

$$\tilde{a}_0 = -\frac{a_{11}\psi_{02}}{\sigma^2}\bar{s}^2 + \frac{3a_{11}\psi_{02}}{\sigma^4}\bar{s} + O(\log(\bar{s})),$$

and

$$\tilde{\psi}_0 = \psi_{02} \left(1 - \frac{a_{11}^2}{\psi_{11}\sigma^2} \right) \bar{s}^2 + \frac{3a_{11}^2\psi_{02}}{\psi_{11}\sigma^4}\bar{s} + O(\log(\bar{s})).$$

4.3 Matching

We now express the inner solution in terms of the outer variable s and expand for small η , so that

$$a_0 = -\frac{a_{11}\psi_{02}}{\sigma^2}s^2 + O(\eta). \quad (43)$$

Similarly, we expand the outer solution in terms of the inner variable for small η . When $\gamma < 1$ we obtain

$$a_0 = -\frac{\lambda B_{ze}}{\sin \lambda}s^2 + \dots \quad (44)$$

Clearly, these solutions match if

$$\psi_{02} = -\frac{\lambda k B_{ze}}{a_{11}\psi_{11} \sin \lambda},$$

and the outer solution (34) is a composite solution to leading order. Again, for the $\gamma > 1$ solutions, substitute Λ for λ into the sinh solutions as for a_1 and ψ_1 . When $\gamma = 1$, we obtain $\psi_{02} = -k B_{ze} / (a_{11} \psi_{11})$. Figure 4 shows numerical solutions to the equations (15) and (16) and the second derivative of a_0 to demonstrate the boundary-layer nature of the solution.

5 Properties of solutions

In this section, figures showing the behaviour of the leading order composite solutions are presented. In cylindrical polar coordinates, in order to find the streamlines of the flux function or stream function, we can use the fact that $RA = \text{constant}$ or $R\Psi = \text{constant}$ along a streamline in a plane of constant ϕ .

5.1 The case $\gamma = 1$

Consider first the case where $\gamma = 1$, so that

$$\begin{aligned} a_1 &= 2B_{Re}s, & \psi_1 &= 2v_{Re}s, \\ a_0 &= -B_{ze}s^2, & \psi_0 &= -v_{ze}s^2, \end{aligned}$$

which, when converted back to the original variables, gives

$$\begin{aligned} A_1 &= B_{Re}R, & \Psi_1 &= v_{Re}R, \\ A_0 &= -\frac{1}{4}B_{ze}R^3, & \Psi_0 &= -\frac{1}{4}v_{ze}R^3, \end{aligned}$$

and so the magnetic flux function (A) and the stream function (Ψ) are

$$A = -\frac{1}{4}B_{ze}R^3 \sin \phi + B_{Re}Rz, \quad \Psi = -\frac{1}{4}v_{ze}R^3 \sin \phi + v_{Re}Rz,$$

with magnetic field and velocity components

$$\begin{aligned} B_R &= B_{Re}R, & B_z &= B_{ze}R^2 \sin \phi - 2B_{Re}z, \\ v_R &= v_{Re}R, & v_z &= v_{ze}R^2 \sin \phi - 2v_{Re}z. \end{aligned}$$

The above condition for streamlines then gives us

$$z = \alpha_1 R^2 \sin \phi + \frac{c_1}{R^2}, \tag{45}$$

where $\alpha_1 = B_{ze}/(4B_{Re})$ or $v_{ze}/(4v_{Re})$ and c_1 is a constant.

The solution (45) is plotted in figure 5, with $c_1 = 0.02, 0$ or -0.02 . These show the field or flow lines within the cylinder contained by $R = 1$ and $-1 < z < 1$. The field lines point radially out from the centre, when $B_{Re} > 0$, coming up or down the spine first when $c_1 \neq 0$ and the flow lines point radially into the centre along the fan, when $v_{Re} < 0$, and then going up or down the spine.

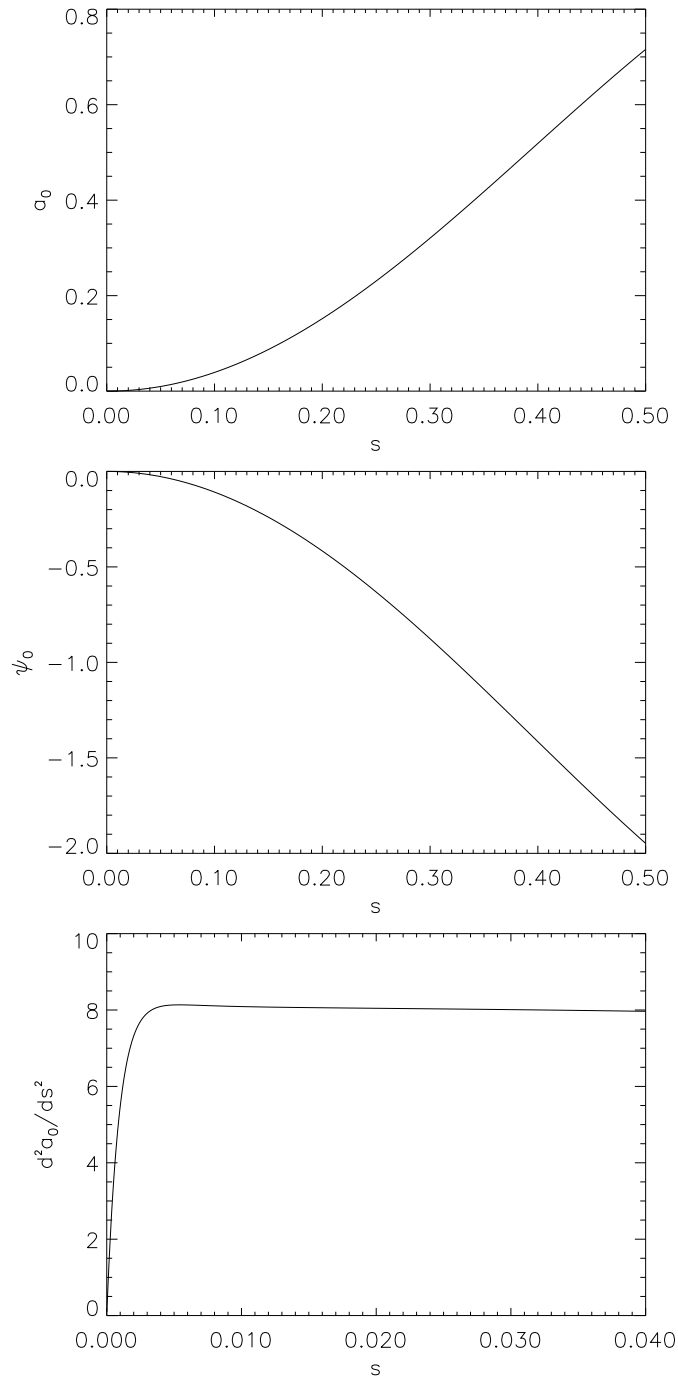


Figure 4: (*Top*) a_0 as a function of s . The parameters are the same as previously, with $v_{ze} = 5$ also. (*Middle*) ψ_0 as a function of s . The parameters are the same as previously. (*Bottom*) $d^2 a_0 / ds^2$ as a function of s with $\eta = 0.01$ displaying the boundary-layer nature of the solution.

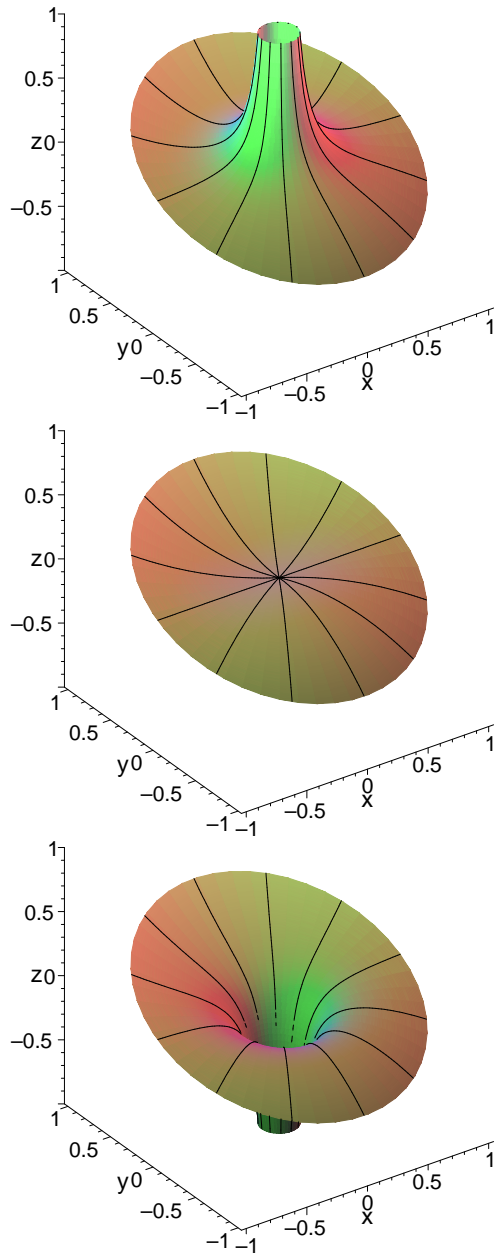


Figure 5: (*Top*) Streamlines for the case $\gamma = 1$ and $c_1 = 0.02$. (*Middle*) Streamlines for the case $\gamma = 1$ and $c_1 = 0$. (*Bottom*) Streamlines for the case $\gamma = 1$ and $c_1 = -0.02$.

5.2 The case $\gamma < 1$

Now consider the case where $\gamma < 1$, so that

$$a_1 = B_{Re} \frac{\sin(2\lambda s)}{\sin \lambda}, \quad \psi_1 = v_{Re} \frac{\sin(2\lambda s)}{\sin \lambda},$$

$$a_0 = \frac{B_{ze}}{2\lambda \sin \lambda} (\cos(2\lambda s) - 1), \quad \psi_0 = \frac{v_{ze}}{2\lambda \sin \lambda} (\cos(2\lambda s) - 1),$$

which, in terms of the original variables becomes

$$A_1 = B_{Re} \frac{\sin(\lambda R^2)}{R \sin \lambda}, \quad \Psi_1 = v_{Re} \frac{\sin(\lambda R^2)}{R \sin \lambda},$$

$$A_0 = \frac{B_{ze}}{2\lambda \sin \lambda} \frac{(\cos(\lambda R^2) - 1)}{R}, \quad \Psi_0 = \frac{v_{ze}}{2\lambda \sin \lambda} \frac{(\cos(\lambda R^2) - 1)}{R},$$

and so the magnetic flux function (A) and the stream function (Ψ) are

$$A = \frac{B_{ze}}{2\lambda \sin \lambda} \frac{(\cos(\lambda R^2) - 1)}{R} \sin \phi + B_{Re} \frac{\sin(\lambda R^2)}{R \sin \lambda} z,$$

$$\Psi = \frac{v_{ze}}{2\lambda \sin \lambda} \frac{(\cos(\lambda R^2) - 1)}{R} \sin \phi + v_{Re} \frac{\sin(\lambda R^2)}{R \sin \lambda} z,$$

with magnetic field and velocity components

$$B_R = B_{Re} \frac{\sin(\lambda R^2)}{R \sin \lambda}, \quad B_z = B_{ze} \frac{\sin(\lambda R^2)}{\sin \lambda} \sin \phi - \frac{2\lambda B_{Re}}{\sin \lambda} \cos(\lambda R^2) z,$$

$$v_R = v_{Re} \frac{\sin(\lambda R^2)}{R \sin \lambda}, \quad v_z = v_{ze} \frac{\sin(\lambda R^2)}{\sin \lambda} \sin \phi - \frac{2\lambda v_{Re}}{\sin \lambda} \cos(\lambda R^2) z.$$

Using the condition for streamlines, we obtain

$$z = \alpha_2 \cot(\lambda R^2) \sin \phi + c_2 \operatorname{cosec}(\lambda R^2), \quad (46)$$

where $\alpha_2 = -B_{ze}/(2\lambda B_{Re})$ or $-v_{ze}/(2\lambda v_{Re})$ and c_2 is a constant.

The solution (46) is shown in figure 6, with $c_2 = 0.08, 0$ or -0.08 . Again, the magnetic field lines point up or down the spine towards the null and radially out along the fan when $B_{Re} > 0$. The flow lines point radially in along the fan and out along the spine when $v_{Re} < 0$.

5.3 The case $\gamma > 1$

Now consider the case where $\gamma > 1$, so that

$$a_1 = B_{Re} \frac{\sinh(2\Lambda s)}{\sinh \Lambda}, \quad \psi_1 = v_{Re} \frac{\sinh(2\Lambda s)}{\sinh \Lambda},$$

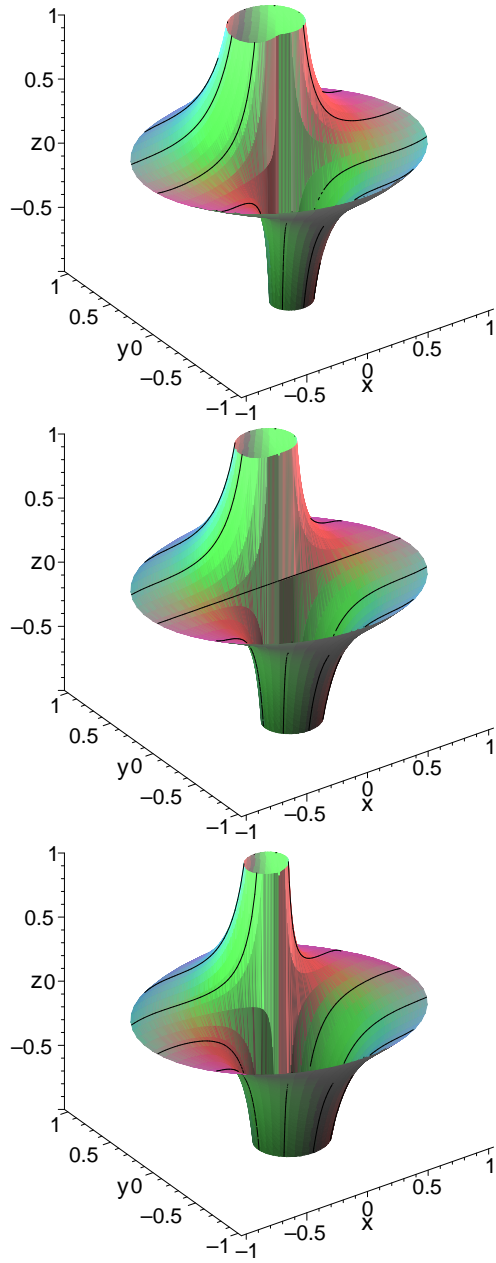


Figure 6: (*Top*) Streamlines for the case $\gamma = 0.45$ and $c_2 = 0.08$. (*Middle*) Streamlines for the case $\gamma = 0.45$ and $c_2 = 0$. (*Bottom*) Streamlines for the case $\gamma = 0.45$ and $c_2 = -0.08$.

$$a_0 = -\frac{B_{ze}}{2\Lambda \sinh \Lambda} (\cosh(2\Lambda s) - 1), \quad \psi_0 = -\frac{v_{ze}}{2\Lambda \sinh \Lambda} (\cosh(2\Lambda s) - 1),$$

or in terms of the original variables,

$$A_1 = B_{Re} \frac{\sinh(\Lambda R^2)}{R \sinh \Lambda}, \quad \Psi_1 = v_{Re} \frac{\sinh(\Lambda R^2)}{R \sinh \Lambda},$$

$$A_0 = -\frac{B_{ze}}{2\Lambda \sinh \Lambda} \frac{(\cosh(\Lambda R^2) - 1)}{R}, \quad \Psi_0 = -\frac{v_{ze}}{2\Lambda \sinh \Lambda} \frac{(\cosh(\Lambda R^2) - 1)}{R},$$

Thus the magnetic flux function (A) and stream function (Ψ) are

$$A = -\frac{B_{ze}}{2\Lambda \sinh \Lambda} \frac{(\cosh(\Lambda R^2) - 1)}{R} \sin \phi + B_{Re} \frac{\sinh(\Lambda R^2)}{R \sinh \Lambda} z,$$

$$\Psi = -\frac{v_{ze}}{2\Lambda \sinh \Lambda} \frac{(\cosh(\Lambda R^2) - 1)}{R} \sin \phi + v_{Re} \frac{\sinh(\Lambda R^2)}{R \sinh \Lambda} z,$$

with magnetic field and velocity components

$$B_R = B_{Re} \frac{\sinh(\Lambda R^2)}{R \sinh \Lambda}, \quad B_z = -B_{ze} \frac{\sinh(\Lambda R^2)}{\sinh \Lambda} \sin \phi - \frac{2\Lambda B_{Re}}{\sinh \Lambda} \cosh(\Lambda R^2) z,$$

$$v_R = v_{Re} \frac{\sinh(\Lambda R^2)}{R \sinh \Lambda}, \quad v_z = -v_{ze} \frac{\sinh(\Lambda R^2)}{\sinh \Lambda} \sin \phi - \frac{2\Lambda v_{Re}}{\sinh \Lambda} \cosh(\Lambda R^2) z.$$

The streamlines in a plane of constant ϕ are

$$z = \alpha_3 \coth(\Lambda R^2) \sin \phi + c_3 \operatorname{cosech}(\Lambda R^2), \quad (47)$$

where $\alpha_3 = B_{ze}/(2\Lambda B_{Re})$ or $v_{ze}/(2\Lambda v_{Re})$ and c_3 is a constant.

The solution (47) is shown in figure 7, with $c_3 = 0.08, 0$ or -0.08 .

6 Comparison of solutions

6.1 The solutions of Craig & Fabling

In dimensional units, the solutions of Craig & Fabling (1) and (2) can be written for our purposes as

$$v_z = -2v_{Re} z + B_{Re} f(R) \sin \phi, \quad v_R = v_{Re} R, \quad (48)$$

$$B_z = -2B_{Re} z + f(R) \sin \phi, \quad B_R = B_{Re} R, \quad (49)$$

where substituting a sine function for a cosine function and setting $m = 1$ loses no generality but allows us to fix an external point at $(x, y, z) = (0, 1, 0)$ where the velocity and magnetic field are \mathbf{v}_e and \mathbf{B}_e to provide a direct comparison with the

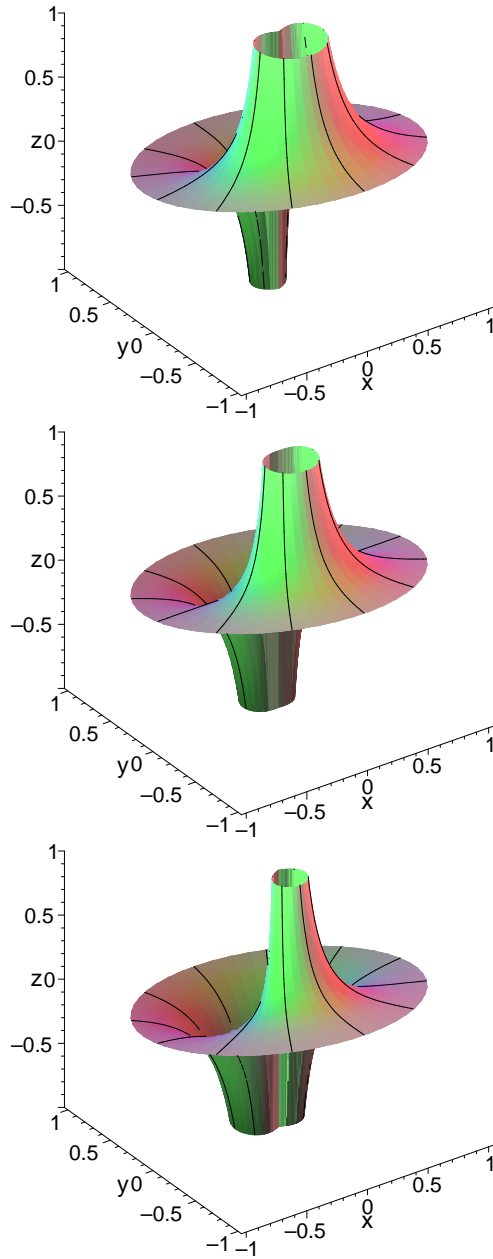


Figure 7: (*Top*) Streamlines for the case $\gamma = 1.8$ and $c_3 = 0.08$. (*Middle*) Streamlines for the case $\gamma = 1.8$ and $c_3 = 0$. (*Bottom*) Streamlines for the case $\gamma = 1.8$ and $c_3 = -0.08$.

generalised solutions in this article. At the external point, we can see that B_{ze}, v_{ze} and B_{Re} are not independent but are related by $B_{ze} = v_{ze}/B_{Re} = f(1)$ in order to satisfy the boundary conditions ($B_R = B_{Re}, v_R = v_{Re}, B_z = B_{ze}, v_z = v_{ze}$) at the external point. In addition, λ and B_{Re} cannot be imposed arbitrarily since the boundary condition on B_R implies that $\lambda = B_{Re}$. This means that we can impose only three of $\lambda, v_{Re}, B_{Re}, v_{ze}$ and B_{ze} . In contrast, the new solutions presented in this article are such that all four of the external boundary conditions can be imposed, as well as the extra parameter, γ . This represents a two-fold generalisation of the Craig-Fabing solutions.

Setting $\gamma = 1$ and explicitly inserting it into (7) and (8), we can see that this reduces to the Craig-Fabing solution as written in (48) and (49), with $\dot{A}_0(R) = -f(R)$ and $\dot{\Psi}_0(R) = -B_{Re}f(R)$ satisfying both (3) and (11).

6.2 Differences between the 2D and 3D cases

Equation (12) has a right-hand side identically equal to zero, whereas the equivalent two-dimensional equation (Priest *et al*, 2000, equation (2.5)) has a non-zero right-hand side. The reason is that the parts of curl of the momentum equation (\mathbf{M}), relating to equation (12), in three dimensions have R and ϕ components of

$$M_R = \frac{\cos \phi}{R} \left(-\Psi_1 \frac{d\dot{\Psi}_0}{dR} + \dot{\Psi}_0 \dot{\Psi}_1 + A_1 \frac{d\dot{A}_0}{dR} - \dot{A}_0 \dot{A}_1 \right), \quad (50)$$

$$M_\phi = (\sin \phi) \frac{d}{dR} \left(\Psi_1 \frac{d\dot{\Psi}_0}{dR} - \dot{\Psi}_0 \dot{\Psi}_1 - A_1 \frac{d\dot{A}_0}{dR} + \dot{A}_0 \dot{A}_1 \right), \quad (51)$$

which are equal to zero, whereas in two dimensions it only has a z -component, namely

$$M_z = \frac{d}{dx} \left(-\psi_1 \frac{d^2 \psi_0}{dx^2} + \frac{d\psi_0}{dx} \frac{d\psi_1}{dx} + A_1 \frac{d^2 A_0}{dx^2} - \frac{dA_0}{dx} \frac{dA_1}{dx} \right), \quad (52)$$

which is also equal to zero. Thus in three dimensions, the R -component (50) gives (12) with the right hand identically zero, while the ϕ -component (51) gives the derivative of (12). In two dimensions, however, the z -component (52) integrates to give equation (2.5).

6.3 The width of the current tube

In order to estimate the width of the current tube extending up the z -axis, we consider $B_z(R, 0)$ which is governed by \dot{A}_0 . In terms of the variables (a, ψ, s) we

may eliminate ψ_0 and ψ_1 from equation (15) using the fact that in the composite solutions for a_1 and ψ_1 there is the relation $\psi_1 = (v_{Re}/B_{Re})a_1$. The result is the following equation for a_0

$$\frac{d^3 a_0}{ds^3} + \left\{ \frac{1}{s} + \frac{K a_1}{2\eta s} \right\} \frac{d^2 a_0}{ds^2} + \left\{ \frac{K}{2\eta s} \frac{da_1}{ds} - \frac{1}{4s^2} \right\} \frac{da_0}{ds} + \frac{C a_1}{\eta s} \frac{da_1}{ds} = 0,$$

where $K = (B_{Re}^2 - v_{Re}^2)/(B_{Re}v_{Re})$ and $C = (B_{Re}B_{ze} - v_{Re}v_{ze})/(B_{Re}v_{Re})$. In order to estimate a length-scale (l) for the width of the spine current, we compare the highest derivative term (which gives rise to the boundary layer) in an order of magnitude way with the second term. In doing so we can make the approximations $s \sim s_0$, $a_1 \sim (2B_{Re}s_0)/\gamma$ and $(d^3 a_0/ds^3)/s_0 \sim (d^2 a_0/ds^2)$ where $s_0 = l^2/2$. To within a numerical factor, we then find the expression

$$s_0 = \frac{\eta\gamma v_{Re}}{B_{Re}^2 - v_{Re}^2},$$

or in terms of the original variables

$$l = \left(\frac{2\eta\gamma v_{Re}}{B_{Re}^2 - v_{Re}^2} \right)^{1/2}.$$

This has exactly the same form as the two-dimensional case when the x -components are replaced by the R -components (Priest *et al*, 2000, equation (5.7)). It can be seen that this represents a scaling of the thickness of the current tube relative to the case $\gamma = 1$ by a factor of $\gamma^{1/2}$. Thus the current tube widens as γ increases or as B_{Re} approaches $|v_{Re}|$. The relationship between l and γ for varying (B_{Re}/v_{Re}) is shown in figure 8.

7 Conclusions

Exact solutions to the nonlinear MHD equations are extremely rare, but are of great value since their properties may be examined in a transparent way and they may give insights about the general physical behaviour of a plasma. In the subject of three-dimensional MHD reconnection only two such solutions have been previously discovered, namely the reconnective fan annihilation regime (Craig *et al* 1995) and the reconnective spine annihilation regime (Craig & Fabling 1996). Here we have presented a two-fold generalisation of the basic spine reconnective annihilation solutions to leading order in η , where η ($\ll 1$) is the dimensionless magnetic diffusivity.

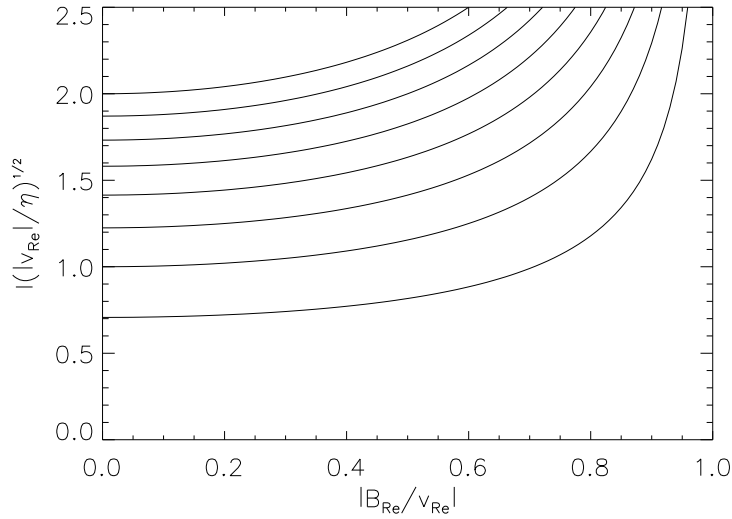


Figure 8: The variation of the current tube width (l) with γ and $|B_{Re}/v_{Re}|$. Starting from 0.25 on the bottom curve, γ increases in steps of 0.25 up to a value of 2 on the top curve.

Acknowledgements

We gratefully acknowledge the financial support from the Volkswagen-Foundation, the Particle Physics and Astrophysics Research Council and the grant of the British-German Research Collaboration. C.M. also wishes to thank Prof. Alan Hood for his invaluable help with numerical integration.

References

- Craig, I. J. D. & Fabling, R. B., “Exact solutions for steady state spine and fan magnetic reconnection,” *Astrophys. J.* **462**, 969-976 (1996).
- Craig, I. J. D., Fabling, R. B., Henton, S. M. & Rickard, G. J., “An exact solution for steady state magnetic reconnection in three dimensions,” *Astrophys. J.* **455**, L197-L199 (1995).
- Craig, I. J. D. & Henton, S. M., “Exact solutions for steady-state incompressible magnetic reconnection,” *Astrophys. J.* **450**, 280-288 (1995).
- Hornig, G. & Rastätter, L., “The magnetic structure of $B \neq 0$ reconnection,” *Physica Scripta* **T74**, 34-39 (1998).
- Lau, Y. -T., & Finn, J. M., “Three-dimensional kinematic reconnection in the presence of field nulls and closed field lines,” *Astrphys. J.* **350**, 672-691 (1990).
- Priest, E. R. & Forbes, T. G., *Magnetic reconnection*, Cambridge University Press

(2000).

Priest, E. R. & Titov, V. S., "Magnetic reconnection of three-dimensional null points," *Phil. Trans. R. Soc. Lond.* **A354**, 2951-2992 (1996).

Priest, E. R., Titov, V. S., Grundy, R. E. & Hood, A. W., "Exact solutions for reconnective magnetic annihilation," *Proc. R. Soc. Lond.* **A456**, 1821-1849 (2000).

Schindler, K., Hesse, M. & Birn, J., "General magnetic reconnection, parallel electric fields and helicity," *J. Geophys. Res.* **93**, 5547-5557 (1988).

Sonnerup, B. U. O. & Priest, E. R., "Resistive MHD stagnation-point flows at a current sheet," *J. Plasma Phys.* **14**, 283-294 (1975).